JOURNAL OF VIROLOGY, Feb. 1995, p. 983–993 Vol. 69, No. 2
0022-538X/95/$04.00+0

Reducing the Complexity of the Transforming Epstein-Barr Virus Genome to 64 Kilobase Pairs

ERLE ROBERTSON AND ELLIOTT KIEFF*

Program in Virology and Department of Medicine and Microbiology and Molecular Genetics, Harvard University, Boston, Massachusetts 02115

Received 16 August 1994/Accepted 20 October 1994

Transformation-competent, replication-defective Epstein-Barr virus (EBV) recombinants which are deleted for 18 kbp of DNA encoding the largest EBNA intron and for 58 kbp of DNA between the EBNA1 and LMP1 genes were constructed. These recombinants were made by transfecting three overlapping cosmid-cloned EBV DNA fragments into cells infected with a lytic replication-competent but transformation-defective EBV (P3HR-1 strain) and were identified by clonal transformation of primary B lymphocytes into lymphoblastoid cell lines. One-third of the lymphoblastoid cell lines were infected with recombinants which had both deletions and carried the EBNA2 and EBNA3 genes from the transfected EBV DNA and therefore are composed mostly or entirely from the transfected EBV DNA fragments. The deleted DNA is absent from cells infected with most of these recombinants, as demonstrated by Southern blot and sensitive PCR analyses for eight different sites within the deleted regions. Cell growth and EBNA, LMP, and BZLF1 gene expression in lymphoblastoid cell lines infected with these recombinants are similar to those in cells infected with wild-type EBV recombinants. Together with previous data, these experiments reduce the complexity of the EBV DNA necessary for transformation of primary B lymphocytes to 64 kbp. The approach should be useful for molecular genetic analyses of transforming EBV genes or for the insertion of heterologous fragments into transforming EBV genomes.

Epstein-Barr virus (EBV) is uniquely efficient in transforming primary human B lymphocytes into long-term lymphoblastoid cell lines (LCLs) and is an etiologic agent of human malignancies (15, 29–32, 37; for reviews, see references 5 and 22). In transformed B lymphocytes, EBV expresses six nuclear proteins (EBNAs), two integral membrane proteins (LMPs), and two small RNAs (EBERs) (for review, see reference 22). Five EBNAs and LMP1 are critical or essential for latent infection or for B-lymphocyte growth transformation, while EBNA3B, LMP2, and the EBERs are fully dispensable for latent infection and growth transformation in vitro (6, 7, 11, 19, 23, 25, 41, 43, 44, 47). The EBV genome is 172 kbp and is composed mostly of genes involved in lytic infection (for review, see references 9 and 22).

A recombinant EBV molecular genetic strategy has recently been developed for the construction of replication-defective transforming viruses deleted for a large EBV DNA segment (33, 45; for review, see reference 20). The strategy uses the P3HR-1 B-lymphoma cell line which is infected with a replication-competent but nontransforming EBV strain (28) to provide lytic replication and recombination functions for the reconstitution and packaging of EBV genomes from overlapping cloned EBV DNA fragments (20, 33, 45). Transfections with five overlapping DNA fragments inclusive of the entire EBV genome resulted in recombinants composed entirely of the transfected DNAs and a larger number of recombinants which had at least one marker specific for the P3HR-1 EBV genome (45). Replication-defective transforming EBV recombinants deleted for a 58-kbp DNA segment were more efficiently reconstituted by transfecting P3HR-1 cells with three cloned EBV DNA fragments (Fig. 1): the *Eco*RI A fragment (EBV genome bp 7315 to 69119 [1, 9]), the *Sal*I EC fragment (bp 63201 to 105296 [1, 9]), and the ESN deletion fragment (bp 95239 to 117609 fused to bp 163415 to 14294 [1, 9]). This deletion removes 46 kbp (bp 117609 to 163415) relative to B95-8 strain EBV DNA, which is the basis for numbering in most databanks (1, 9). All other EBV genomes have 12 kbp of additional DNA at bp 152012 to 152013 (Fig. 1) (9, 12). Recombination among the three transfected cosmids results in a 46-kbp deletion relative to the B95-8 EBV genome and a 58-kbp deletion relative to wild-type (WT) EBV genomes. Transforming EBV recombinants have also been constructed which are deleted for the LMP2 (bp 02 to 648), EBERs (bp 6612 to 7263), BCRF1 (bp 9535 to 12870), and BHRF1 (bp 53721 to 60612) encoding DNA segments (23, 26, 40, 41).

The objective of the experiments described here was to further reduce the complexity of transforming EBV recombinants so as to facilitate molecular genetic analysis of the critical domains of the essential transforming genes. Further significant reductions in the genetic complexity of transforming EBV recombinants beyond the previous 58-kbp deletion is dependent on the deletion of EBV DNA which encodes large introns of the EBNA transcripts. This 100-kbp transcript is initiated at the Wp or Cp promoter, which map at EBV genome bp 14352 and 11305, respectively, and terminates at EBV genome bp 109937 (Fig. 1) (1–4, 9, 18, 34, 35, 39). The largest intron is 25 kbp and extends from bp 67649 to 92670 (Fig. 1). These experiments specifically evaluate whether the DNA encoding this intron could also be deleted without compromising the ability of the resultant recombinant to be packaged or to growth transform primary B lymphocytes.

MATERIALS AND METHODS

Cells and cell culture. Cells were maintained in complete medium consisting of RPMI 1640 supplemented with 10 to 15% inactivated fetal bovine serum, 2 mM glutamine, 10 μg of gentamicin, and 50,000 U of penicillin per ml. The P3HR-1 (16, 29) and B95-8 cell lines were obtained from G. Miller, Yale University.

* Corresponding author. Mailing address: Department of Medicine and Microbiology and Molecular Genetics, Harvard University, 75 Francis St., Boston, MA 02115. Phone: (617) 732-7048. Fax: (617) 732-7099. Electronic mail address: KIEFFE@TNP01.BWH.HARVARD.EDU (Internet).

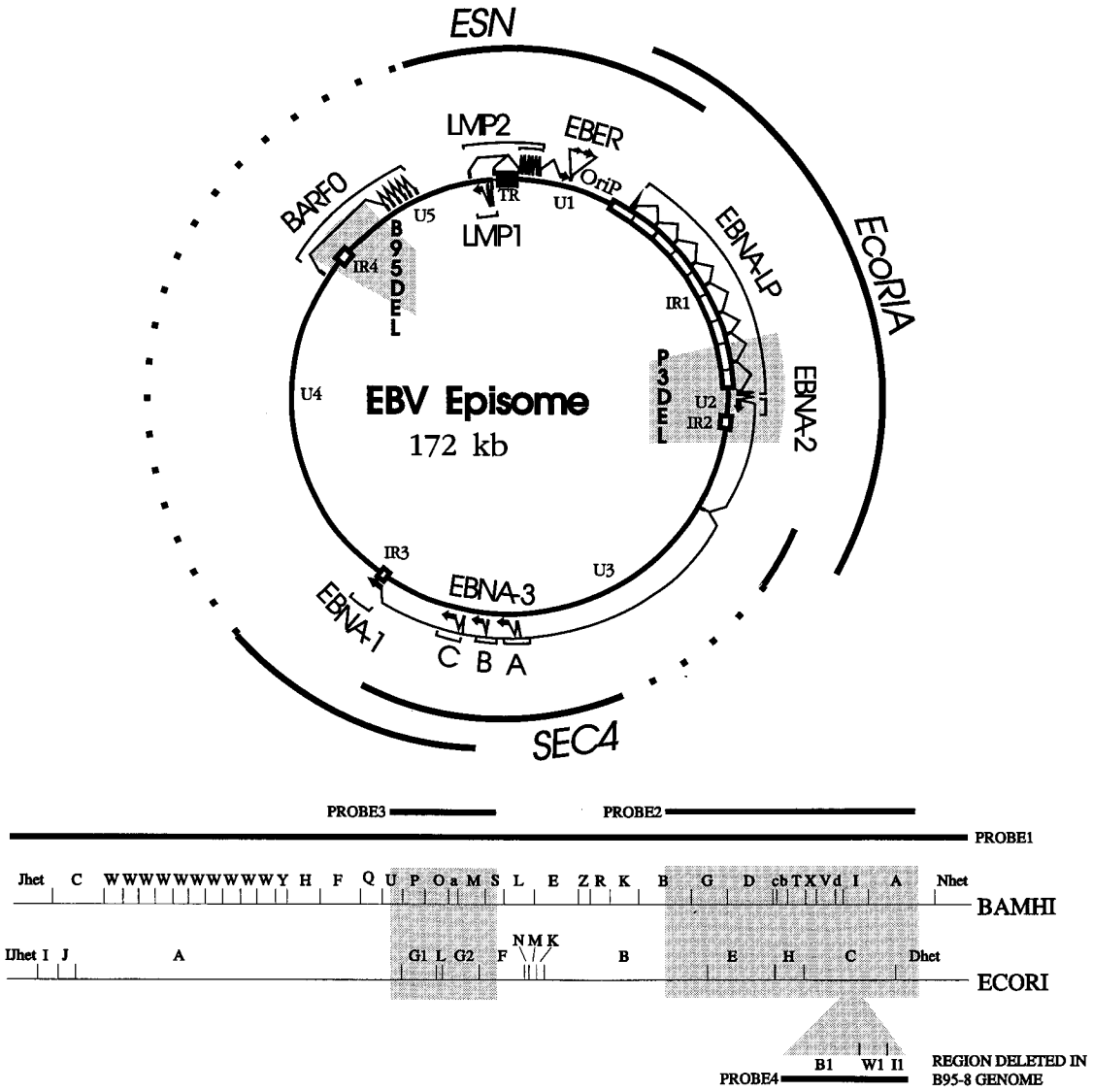

FIG. 1. Schematic diagrams of the EBV genome in circular (top) and linear (bottom) formats, indicating the major transcripts in latent infection (EBNAs, LMPs, and EBERs). The 12-kbp and the EBNALP/2 deletions characteristic of the B95-8 and P3HR-1 EBV strains, respectively, are indicated by shaded areas in the circular map. The unique (U1 to U5) and the internal repeat regions (IR1 to IR4) of the EBV genome are indicated. The *Eco*RI A, *Sal*I E/C 18-kbp deletion cosmid (SEC4) and the 58-kbp *Sna*BI B-*Eco*RI B deletion cosmid (ESN) are shown. The broken lines in the top diagram and the shaded areas in the bottom diagram indicate the 18- and 58-kbp deletions created in these experiments. These deletions correspond to bp 68928 to 87030 and bp 117609 to 163415, respectively (1, 9). The *Bam*HI and *Eco*RI maps are shown for reference to the PCR and Southern blot analyses. The *Bam*HI B1, I1, and W1 fragments, which are partially (B1 and I1) or completely (W1) deleted from the B95-8 genome are indicated as an insert into the *Eco*RI map. There is no *Eco*RI site in the 12 kbp, so that the *Eco*RI C fragment of WT EBV DNA is 12 kbp larger than that of B95-8.

Plasmids, transfection, infection of primary B lymphocytes, and outgrowth of LCLs. The SEC4 cosmid DNA was constructed by deleting the *Rsr*II fragments corresponding to EBV genome bp 68928 to 87030 from *Sal*I EC (42). The ESN cosmid is deleted for EBV genome bp 117609 to 163415 (33). EBV recombinants were prepared by transfection of P3HR-1 cells with cosmid-cloned EBV DNA fragments after releasing the EBV DNA from the vector by restriction endonuclease digestion (42–45). The resultant virus was then used to infect primary B lymphocytes (42–45). The cells were incubated with the virus for 2 h at 37°C and then plated in 96-well microtiter plates in 150 μl of complete medium. LCLs were macroscopically visible 3 to 4 weeks after incubation and expanded thereafter.

PCR. All primers used for PCR were made on an Applied Biosystems model 391 synthesizer. The primers used to detect the SEC4 deletion correspond to bp 68821 to 68845 and 87197 to 87173, which amplify a DNA product of 274 bp across the deletion, and the primers used to detect the ESN deletion correspond to bp 117520 to 117543 and 163595 to 163578, which amplify a 269-bp DNA product across the ESN deletion (1, 33). The primer pairs used to detect specific regions within the deletions are described in Table 2, and the sizes of the PCR products are given in the figure legends. The sensitivity of the WT primers was tested by serial dilution of the WT LCL DNA in DNA prepared from an EBV-negative Burkitt's lymphoma cell line, BJAB (33). The EBV copy number in P3HR-1 cells was estimated by PCR of endpoint-diluted P3HR-1 cells relative to Namalwa cells (2 copies of the EBV genome per cell [14, 27]). The P3HR-1 cells were serially diluted in BJAB cells so that the total cell DNA remained constant.

Immunoblot, Southern blot, and in situ lysis cell gel analysis. The EBV proteins were denatured in lysis buffer by boiling for 5 min and were separated on denaturing 8% polyacrylamide–sodium dodecyl sulfate (SDS) gels. Latent and early lytic EBV antigens were detected by immunoblot with EBV immune sera (33) or with S12 monoclonal antibody to LMP1 (24). Southern and in situ lysis (10) analyses have been described before (33).

RESULTS

LCLs transformed by EBV recombinants deleted for 18 kbp encoding most of the largest EBNA intron and for 58 kbp

between the EBNA1- and LMP1-encoding DNAs. The strategy to construct EBV recombinants deleted for DNA encoding most of the major EBNA intron uses three overlapping cosmid clones of EBV DNA: WT *Eco*RI A (bp 7315 to 69119), an 18-kbp deletion clone, SEC4 (bp 63201 to 68928 fused to bp 87030 to 105296), and a 58-kbp deletion clone, ESN (bp 95239 to 117609 fused to bp 163415 to 14294) (Fig. 1) (1, 33). These cosmids were transfected into P3HR-1 cells along with an expression plasmid for the Z transactivator of EBV replication. The resultant virus was used to infect primary B lymphocytes, and the infected cells were plated at an expected endpoint dilution for outgrowth of cells infected with a transforming virus (33).

If the deletion of DNA encoding the EBNA intron had no effect on the ability of recombinants constituted from only the transfected cosmid DNAs to replicate, recombine, be packaged into virus, and initiate latent infection and cell growth transformation, about half of the LCLs which arose would be expected to be infected with such recombinants (33). The remainder would be infected with recombinants which had recombined with the endogenous P3HR-1 EBV genome (33). If the deletion of both regions of the genome had an adverse effect, a small fraction or none of the LCLs would be infected with a recombinant comprised solely of transfected cosmid EBV DNA. However, some LCLs could arise which were infected with the recombinant EBV containing both deletions even if there were an adverse effect on expression of the essential downstream EBNAs (EBNA3A, -3B, -3C, and -1; see Fig. 1) since a significant fraction of the LCLs which are produced following infection with EBV recombinants produced from P3HR-1 cells are coinfected with a recombinant and with nonrecombinant P3HR-1 EBV. The parental P3HR-1 virus is produced in 10^5-fold excess over recombinants and can provide EBNA3s, EBNA1, or LMP1 in *trans* (20, 33, 42–45).

The genotype of the EBV in the resultant LCLs was initially evaluated by three sets of PCR analyses with primers specific for the 58-kbp deletion characteristic of the ESN cosmid, for the 18-kbp EBNA intron deletion characteristic of the SEC4 cosmid, or for the EBNA3A gene, which differs between the transfected type 1 B95 EBV DNA fragments and the type 2 P3HR-1 EBV (36) (Fig. 1 to 6). All recombinants must have the EBNALP/2 genes of the transfected EBV *Eco*RI A DNA fragment, since P3HR-1 lacks this DNA segment and restoration of that deletion is essential for primary B-lymphocyte growth transformation (12, 17, 21, 28, 38).

The EBV genotype of 87 recombinant-infected LCLs was evaluated (Table 1). The largest group of LCLs, 32 of 87, were infected with a recombinant that had the deletion markers from both of the transfected EBV DNAs. Of the 32 which had incorporated both deletions, 31 had the type 1 EBNA3A gene of the transfected EBV DNA and therefore appeared, on the basis of all four markers (the three indicated in the table and the EBNALP/2 DNA, essential for marker rescue of transformation in the P3HR-1 system), to comprise solely the transfected EBV cosmid DNA. Only 7 of these 31 LCLs were coinfected with P3HR-1 EBV, as indicated by the presence of both type 1 EBNA3A DNA from the transfected DNA and type 2 EBNA3A from the P3HR-1 EBV genome (Table 1).

Representative PCRs with primer pair B1 and B2 (Table 2, Fig. 2B) result in the amplification of a 276-bp fragment from the transfected type 1 B95-8 EBNA3A DNA or a 237-bp fragment for the type 2 P3HR-1 EBV DNA (Fig. 2). Only the type 1 EBNA3A DNA is detected in LCLs infected with most EBV recombinants that have both deletions (Fig. 2).

The second largest group, 23 of 87, were infected with a recombinant that had the 18-kbp deletion but not the 58-kbp deletion. The third largest group, 21 of 87, were simple recombinants between the transformation marker rescuing the EBNALP/2 EBV DNA fragment and P3HR-1 EBV. The smallest group, 11 of 87, were infected with a recombinant that was deleted for the 58-kbp segment but not for the 18-kbp segment. Thus, as in the previous experiment, in which the transfected *Sal*I EC fragment was intact (33), most (32 of 43) of the transforming recombinants that had incorporated the 58-kbp deletion also incorporated the other transfected EBV DNA fragments without recombining with the P3HR-1 EBV and without a requirement for P3HR-1 EBV in order to enable growth transformation of cells as LCLs (Table 1). The finding that 24 of 87 LCLs are infected with a recombinant EBV that has both deletions and only the type 1 EBNA3A gene is an initial indication that the two deletions do not impair the ability of the recombinant to transform primary B lymphocytes. The analyses described below more rigorously exclude any WT DNA in LCLs infected with the EBV recombinants deleted for both regions of the genome.

TABLE 1. EBV genotypes in transformed LCLs

Deletion[a]	No. of LCLs			
	Total	Type 1 EBNA3A	Type 2 EBNA3A	Types 1 and 2 EBNA3A[b]
Neither	21	2	21	2
18 kbp	23	10	16	3
58 kbp	11	6	9	4
18 kbp + 58 kbp	32	31	8	7
Total	87	49	54	16

[a] Refers to the deletion at the specific sites indicated.
[b] Indicates coinfection with nonrecombinant P3HR-1.

Absence of WT EBV DNA from LCLs infected with EBV recombinants deleted for 18 and 58 kbp of the genome. PCR analyses were done to investigate at a high level of sensitivity whether the LCLs infected with 18- and 58-kbp-deleted EBV recombinants have incorporated the putatively deleted DNA at another site. For each deletion, the analyses would detect one copy of any of four separate segments of the deleted DNA

TABLE 2. Primers used in EBV genome analysis

Primer	Sequence (5′–3′)	Coordinates (bp)
A1	AGA GCA GGT CGG TCA GGC GTC	68821–68845
A2	GAG AGT TCC ATA AGC ACC TGG	68999–68978
A3	GGA CGC GGA CGG CGT CAA AGC	87197–87173
A4	TGG GCA GCT CGT TGG AGA GGA	73376–73397
A5	CAT CCG AAC TCC TCA GGT CTC	73658–73679
A6	CTT CTA CAG CAT AGC CCT GCT	79382–79403
A7	GGT GTG CCA TAC AAG GGA GCC	79682–79703
A8	ATC TCC CAG ACT GGT CGT GCT	86934–86954
B1	GAA ACC AAG ACC AGA GGT CC	93596–93665
B2	TCC CAG GGC CGG ACA ATA GG	93871–93852
C1	CTA GTG GCT CCT CTG AAG GAT GG	117520–117543
C2	CTC AGA CAC GCG ACG GGC ACT CGG	117677–117653
C3	GAC CGG AAC CAA CGG TCC	163595–163578
C4	TAC CCA TGT TCG GTG CGA GCC	125185–125206
C5	CGG GCT TGT GCT TGT ACT GAC	125437–125416
C6	TCG GGG ATA CTA TGC AGG ATC	137030–137051
C7	TCA TAG CTT TGA CCT GCT GGT	137366–137345
C8	CGA GAT CAC ATA GGG GTC CCT	163298–163319

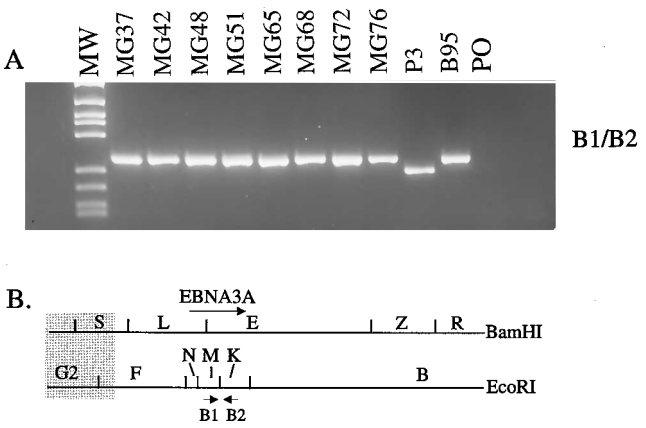

FIG. 2. (A) PCR analysis of recombinant-EBV-infected LCLs using primers which amplify a 276-bp fragment from the transfected type 1 B95-8 EBNA3A DNA or a 237-bp fragment from the type 2 P3HR-1 EBNA3A DNA. DNA molecular weight (MW) markers are *Rsa*I-digested ϕX174 DNA. Lanes MG37 to MG76 are the PCR products of the indicated recombinant LCL DNAs. P3 and B95 are the DNA products amplified from P3HR-1 or B95-8 EBV-infected cell lines, and PO shows no amplification from primers without added EBV DNA. (B) Map location of the B1 and B2 primer pair (defined in Table 2).

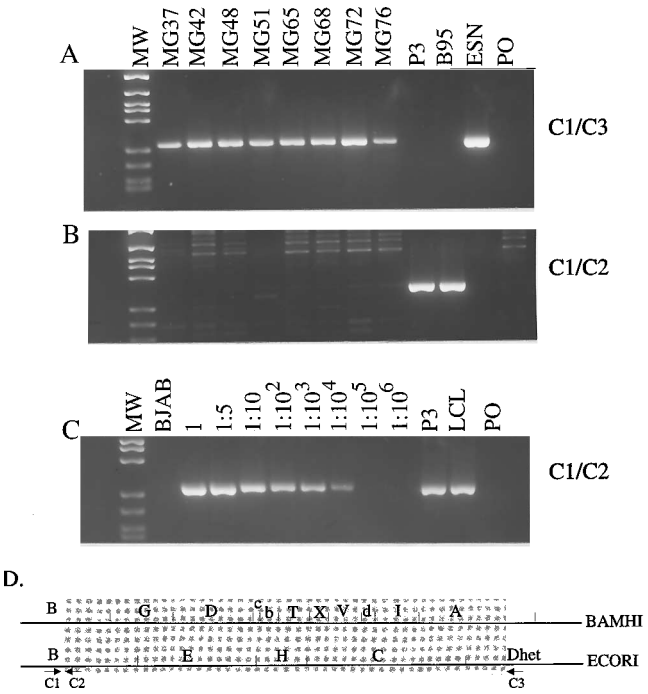

FIG. 3. PCR analyses for the 58-kbp deletion in recombinant-EBV-infected LCLs. (A) Primers C1 and C3 result in the amplification of a 269-bp fragment across the site of the 58-kbp deletion with DNA from LCLs MG37 to MG76 or from 10 ng of the transfected 58-kbp deletion ESN cosmid DNA. No fragment is amplified from B95-8- or P3HR-1-infected cells or with primers and no DNA added. (B) PCR analyses with primers C1 and C2, which amplify a 157-bp WT DNA fragment from P3HR-1 or B95-8 EBV DNA and no amplification product from the MG37 to MG76 LCLs. (C) Sensitivity of the C1 and C2 primers for WT DNA within the 58-kbp deletion using WT-infected LCL DNA serially diluted in DNA from an EBV-negative B-cell line, BJAB. The DNA molecular weight markers (lanes MW) are *Rsa*I-digested ϕX174 DNA. Lanes P3 and B95 are P3HR-1- and B95-8-infected cells, respectively. (D) Map location of the PCR primers (defined in Table 2) in relation to the 58-kbp ESN deletion (shaded area).

at a sensitivity of 1 EBV genome per 100 cells. The primers used in these analyses are described in Table 2, and Fig. 3 to 6 show examples of the results and the location of each primer relative to the deletion on the EBV genome. Examples of eight LCLs are shown. The expected 269-bp fragment is amplified from all eight LCLs with the C1 and C3 primer pair, which flank the 58-kbp deletion (Fig. 3A, 3D, 4A, and 4E). This demonstrates the absence of WT DNA at the site of the 58-kbp deletion in these LCLs. Using the C1 and C2 primer pair, which is specific for WT DNA at one of the sites within the deletion, the expected 157-bp fragment was readily detected with P3HR-1- or B95-8-infected cell DNA and not in the LCLs infected with EBV recombinants deleted for both regions of the genome (Fig. 3B to D). The detection of WT DNA for the 58-kbp deletion with the latter primer pair was sufficiently sensitive that the presence of one WT copy of the DNA in 10^4 cells would have been detected (Fig. 3B and C). These data therefore exclude the deleted DNA from being in the transformed cells as a result of P3HR-1 coinfection or incorporation at another site in the transforming EBV recombinant genomes.

Further analysis using three other PCR primer pairs specific for three other sites in the 58-kbp deletion demonstrated that these DNAs were also absent from the LCLs infected with putative 18- and 58-kbp-deleted EBV recombinants (Fig. 4B to E; see Table 2 for coordinates). Each of these primer pairs would detect 1 EBV molecule in every 100 cells (Fig. 4B to D). PCR with WT-infected-cell DNAs amplified 252-bp, 336-bp, and 297-bp fragments with primer pairs C4 and C5, C6 and C7, and C8 and C3, respectively, and no fragment was amplified from the LCLs infected with the transforming mini-EBV recombinants (Fig. 4B to E).

Similarly, a 274-bp fragment characteristic of the 18-kbp deletion was readily detected in each of the LCLs using primer pair A1 and A3 (Fig. 5A). Each of the LCL DNAs failed to amplify a 178-bp WT PCR DNA product with primer pair A1 and A2, which would detect 1 WT DNA molecule in 10^4 cells at this site (Fig. 5B and C). PCR analyses for detection of WT DNA at three other sites within the 18-kbp deletion demonstrated the absence of WT DNA at these three other positions as well (Fig. 6). Using primer pairs A4 and A5, A6 and A7, and A8 and A3, PCR DNA fragments of 303, 321, and 263 bp, respectively, were amplified, for WT DNA at these three sites, and no DNA product was amplified from the LCLs infected with the transformation-competent EBV recombinant genomes (see Table 2 and Fig. 6B to E). These primer pairs would detect 1 WT EBV molecule in 100 cells. These data therefore exclude the presence of four separate sites in the 18-kbp deletion and of four separate sites in the 58-kbp deletion.

Southern blot analyses of the recombinant EBV DNA. DNA from each of seven LCLs infected with the 18-kbp- and 58-kbp-deleted minitransforming EBV recombinants was digested with *Eco*RI, *Sal*I, or *Bam*HI restriction endonuclease, transferred to filters, and probed with each cosmid EBV DNA fragment separately, with an *Mlu*I-*Eco*RI DNA fragment that contains the terminal repeats, with total EBV DNA, with the DNA which had been deleted from the two transfected EBV DNA fragments, or with DNA specific for the 12 kbp of WT DNA for which the B95-8 genome is naturally deleted. The data are of similar quality, and only the data from the *Eco*RI and the *Bam*HI digests probed with total EBV DNA or with the DNA deleted from the LCLs are shown (Fig. 7 to 9). Most of the EBV DNA fragments in these seven LCLs and all of the fragments in four of these LCLs were only those expected from simple homologous recombination among the three transfected cosmid EBV DNA fragments. WT probe DNA specific for the 18-kbp or the 58-kbp deletion hybridized to B95-8 and

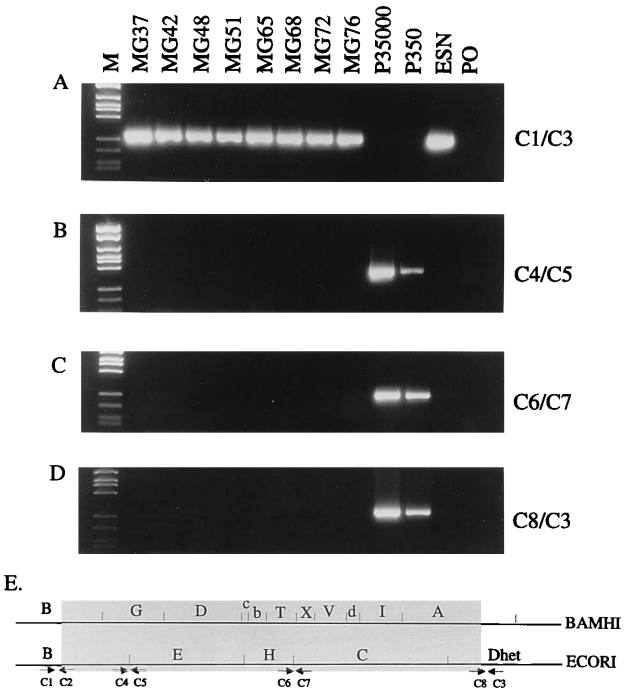

FIG. 4. PCR analyses to detect WT DNA within the 58-kbp deletion. PCR primers C1 and C3 amplify a 269-bp fragment across the deletion using DNA from the LCLs MG37 to MG76 or 10 ng of the ESN deletion cosmid DNA diluted in BJAB cell DNA. Lanes P35000 and P350 are amplifications from 5,000 and 50 P3HR-1 EBV genomes diluted with BJAB cell DNA, respectively. The number of EBV genomes in the P3HR-1 DNA was determined by endpoint dilution relative to Namalwa cell DNA. Namalwa cells have one EBV genome integrated into a chromosome site, which then duplicated. Primers C4 and C5 (B), C6 and C7 (C), and C8 and C3 (D) amplify DNA fragments of 252, 336, and 297 bp, respectively, from 5,000 or 50 copies of P3HR-1 DNA. No amplification product results from LCL DNAs. (E) PCR primers on the B95-8 *Bam*HI and *Eco*RI fragment maps. The primer pair used in each reaction is indicated on the right, and the DNA markers are ϕX174 DNA digested with *Rsa*I. The primers are defined in Table 2. PO, control reaction without added DNA.

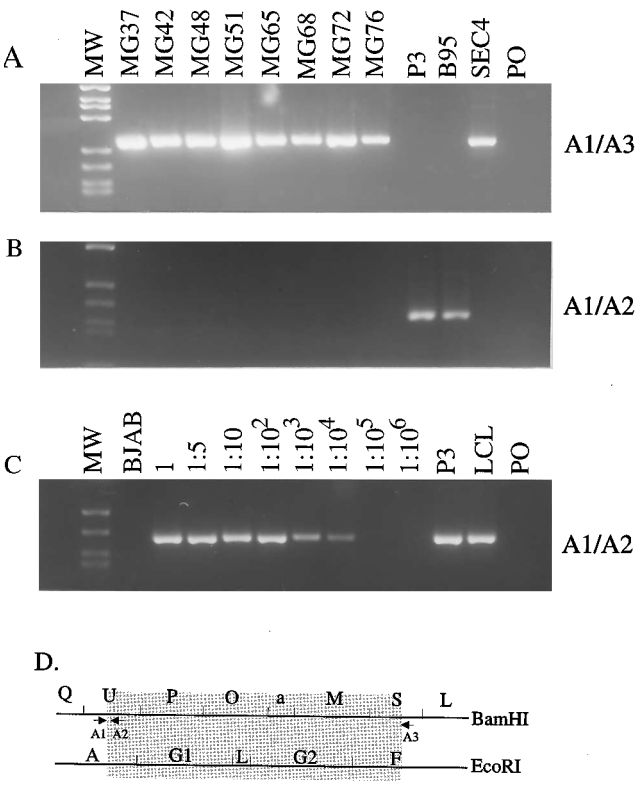

FIG. 5. PCR analyses of recombinant EBV-infected LCLs for the 18-kbp deletion. (A) Primers A1 and A3 result in the amplification of a 274-bp fragment across the site of the 18-kbp deletion with DNA from recombinant-EBV-infected LCLs MG37 to MG76 or 10 ng of SEC4 DNA in BJAB cell DNA. No amplification product results from P3HR-1- or B95-8-infected cells or from an amplification without added DNA (lane PO). (B) Primers A1 and A2 result in the amplification of a 178-bp fragment from WT EBV DNA within the deletion at this site, but a similar fragment is not amplified from LCLs MG37 to MG76. (C) Sensitivity of the primers for WT DNA within the 18-kbp deletion using DNA from a WT latently infected LCL that has 10 EBV genomes per cell. The WT-infected LCL DNA was serially diluted in DNA from an EBV-negative Burkitt's lymphoma cell line, BJAB (33). DNA size markers (lanes MW) are ϕX174 DNA digested with *Rsa*I. (D) Positions of the PCR primers on an EBV genome map in relation to the SEC4 cosmid 18-kbp deletion (shaded area). The primers used in each panel are indicated to the right and are defined in Table 2.

P3HR-1 EBV DNA but not to the LCL DNAs containing the transforming EBV recombinant genomes deleted for 18 kbp or for 58 kbp (see Fig. 7 to 9). For example, an autoradiogram of a blot of *Eco*RI digests probed with total EBV DNA reveals the expected *Eco*RI A and F and *Eco*RI B and Dhet fusion fragments which result from the 18-kbp and 58-kbp deletions, respectively. The normal *Eco*RI I/Jhet, K, and M fragments which are unaffected by the deletions are evident in each LCL (see map in Fig. 1 and Fig. 7A; data not shown for other probes). The terminal repeat-specific probe hybridized to the nondeleted part of the Dhet fragment fused to *Eco*RI B in each of the recombinant-infected LCLs (not shown). As expected, *Eco*RI B, C, E, and H are evident in B95-8 and PHR-1 DNA, and these fragments are not present in the recombinant-infected LCLs probed with the 58-kbp-deleted DNA (Fig. 1 and 7C). Similarly, the *Eco*RI F, G1, G2, and L fragments of P3HR-1 and B95-8 DNA are evident with the 18-kbp-deleted DNA probe, but these fragments are missing from the LCLs infected with the mini-transforming genome. These fragments are not part of any other fragment (Fig. 1 and 7B). The 18-kbp deletion probe also includes a part of *Eco*RI A, and this part of the *Eco*RI A fragment is also missing from the recombinant EBV-infected LCLs (Fig. 1 and 7B).

Some anomalous fragments were also detected in four of the seven LCLs. MG48 and MG72 cells have normal-size and smaller fragments which hybridized to *Eco*RI A probes. The smaller fragments are indicated by a solid dot in Fig. 7A. Since deletions in *Eco*RI A occur during propagation in *Escherichia coli*, the smaller *Eco*RI A fragments may have been present in the transfected DNA and recombined with the overlapping flanking cosmids. Alternatively, since these cells also have a "normal-size" *Eco*RI A, the deletion could have occurred during replication and recombination in P3HR-1 cells or after infection of the primary B lymphocyte. MG68 cells have both the expected *Eco*RI B-Dhet fusion fragment and a smaller fusion fragment (indicated by a solid arrowhead in Fig. 7A), both of which hybridize to a terminal repeat-specific probe. MG65 cells also have the expected *Eco*RI B-Dhet fusion fragment and a slightly smaller *Eco*RI B-Dhet fragment which does not hybridize to the terminal repeat probe (indicated by an arrow in Fig. 7A).

Further illustrative data are shown in the Southern blots of *Bam*HI digests of the same cell DNAs in Fig. 8. A total-EBV-genome probe has been used in Fig. 8A, and the fragments are labeled according to the maps shown in Fig. 1. Each of the LCLs infected with a double deletion recombinant lacks a *Bam*HI A fragment, which is the largest fragment evident in

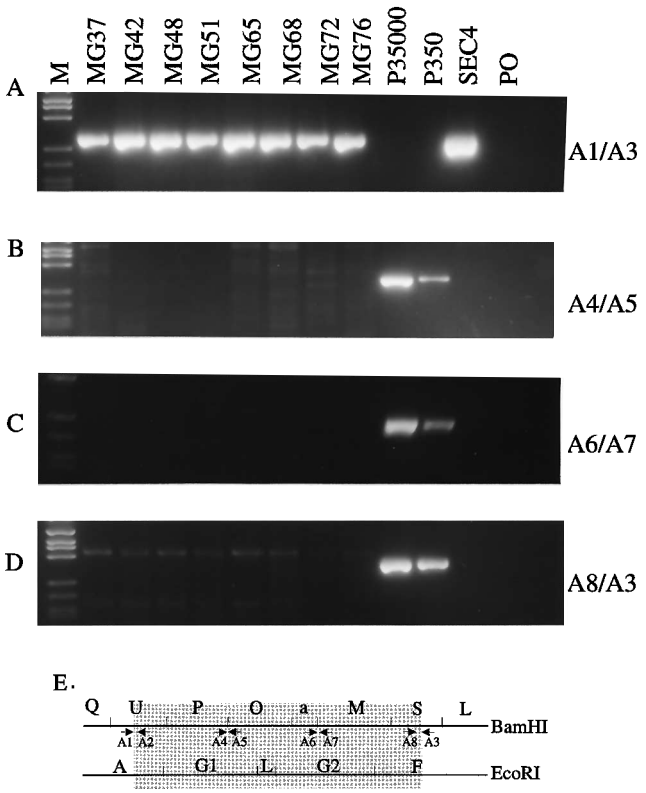

FIG. 6. PCR analyses to detect WT DNA within the 18-kbp deletion. (A) PCR primers A1 and A3 amplify a 274-bp fragment across the deletion using DNA prepared from LCLs MG37 to MG76 or 10 ng of SEC4 DNA diluted in DNA from BJAB cells. Lanes P35000 and P350 are 5,000 and 50 P3HR-1 EBV genomes diluted in BJAB cell DNA, respectively. The amount of EBV DNA in P3HR-1 cells was determined by endpoint dilution PCR relative to Namalwa cells DNA as described in the legend to Fig. 4. Primers A4 and A5 (B), A6 and A7 (C), and A8 and A3 (D) amplify 303-bp, 321-bp, and 263-bp DNA fragments, respectively, from WT DNA within the deleted region. (E) Positions of primers within the EBV genome in relation to the deleted region (shaded). The primer pair used in each reaction is shown on the right and defined in Table 2. Lane M, ϕX174 DNA digested with *Rsa*I. PO, primer-only control reaction.

the B95-8 digest, but is mostly deleted from the recombinant-infected LCLs as a consequence of the 58-kbp deletion. Instead, the largest fragment in each LCL is a fusion fragment between the ends of the linear EBV DNA as a consequence of episome formation. This latter fragment, marked on the right by a solid circle in Fig. 8A, was specifically identified because it hybridized to the terminal repeat probe (data not shown). The next largest fragments in the B95-8 digest are *Bam*HI B and C, which at 9.7 and 9.2 kbp are not well separated. In the P3HR-1 genome, the *Bam*HI site between B and G is absent, resulting in a BG fusion fragment which is the largest P3HR-1 *Bam*HI fragment. P3HR-1 also has a B1 fragment which is not present in B95 DNA because of a deletion from the B95-8 genome (see map in Fig. 1). The *Bam*HI B and B1 fragments are missing from all of the recombinant-infected LCLs as a consequence of the 58-kbp deletion (Fig. 8C). The *Bam*HI C fragment is present in the recombinant-infected LCLs and can be seen as a fragment similar in size to the more rapidly migrating component of the *Bam*HI B and C complex. The *Bam*HI C fragment is most evident in the MG68 lane because of the very large size of the episomal *Bam*HI fused-end fragment and the higher EBV genome copy number in the MG68 DNA. The next largest B95-8 fragments are *Bam*HI D, E, and F. The *Bam*HI D fragment is deleted from each of the recombinant-infected LCLs as a consequence of the 58-kbp deletion (Fig. 8C). The DE and F band in Fig. 8A, however, is still intense since a new fusion fragment has resulted from the left 5 kbp of *Bam*HI B being joined to the right 3.2 kbp of *Bam*HI A (see Fig. 1). This new fusion was specifically identified in other blots with an ESN-specific probe (data not shown). *Bam*HI G and H are 6.5 and 6.0 kbp, not clearly separated in the B958 lane, and both absent from the P3HR-1 lane (G is fused to B in P3HR-1, and H is largely deleted from P3HR-1). In most of the recombinant-infected LCLs, *Bam*HI H is evident as a band equal in size to the top of the G band, probably because of an expansion in the number of repeats in this fragment. *Bam*HI I is intensely identified in the B95 lane. *Bam*HI I is absent from the recombinant-infected LCLs as a consequence of the 58-kbp deletion (Fig. 8C). Other *Bam*HI fragments which are evident in B95, P3HR-1, and each of the recombinant-infected LCLs are K and L (an intense band which in the B95 and P3HR-1 lanes includes hybridization to the M fragment), Q and R (two clearly separated bands evident in each of the recombinant-infected LCLs and partially obscured in the B958 and P3HR-1 digests by the O, P, S, T, and U fragments which are deleted from the recombinant-infected LCLs), and *Bam*HI Y and Z, which are 1.85 and 1.8 kbp, respectively. Probe 3, which is specific for the 18-kbp deletion DNA, hybridizes to the expected (see maps in Fig. 1) *Bam*HI M, O, P, S, and U and a fragment of B95-8 and P3HR-1 DNA and to no fragments in the recombinant-EBV-infected LCLs (Fig. 8B). Probe 2, which is specific for the 58-kbp deletion, also hybridizes to the expected fragments of B95-8 and P3HR-1 DNA and to no fragments in the recombinant-EBV-infected LCL DNAs (Fig. 1 and 8C).

A probe was then made from the EBV DNA *Bam*HI B1, I1, and W1 fragments since these include the 12 kbp of DNA missing from the B95-8 strain. This probe was hybridized to blots of P3HR-1, B95-8, and the transforming EBV-recombinant-infected LCL DNAs to be certain that anomalous events had not resulted in incorporation of this segment from the P3HR-1 EBV DNA into the recombinant genomes. The probe hybridizes to the expected (Fig. 1) *Eco*RI C* and C fragments of P3HR-1 and B95-8 DNA, respectively, to the *Bam*HI B1, I1, and W1 fragments of P3HR-1 DNA, and to the *Bam*HI I fragment of B95-8 DNA. Since *Bam*HI B1 also has partial homology to the *Bam*HI H fragment (12), faint hybridization is seen to *Bam*HI H and to *Eco*RI A in B95-8, P3HR-1, and each of the recombinant-infected LCLs. The probe did not hybridize to any other fragment in any of the 18- and 58-kbp-deleted recombinant-EBV-infected LCLs (Fig. 9; other data not shown). Thus, these and the previous data demonstrate that the 18-kbp- and the 58-kbp-deleted DNAs are absent from the 18- and 58-kbp recombinant-EBV-infected cells.

EBV episomes in recombinant-EBV-infected LCLs. The size and abundance of EBV episomes in LCLs transformed by double-deletion EBV recombinants were compared with the episomes in cells infected with the P3HR-1 and B95-8 EBV strains (Fig. 10). In each of the multiple in situ lysis gel analyses that were done (because of varying degrees of incomplete in situ lysis), the abundance of episomes in cells infected with the recombinants was similar to that in P3HR-1- or B95-8-infected cells. The size of the episomes in some of the double-deletion EBV-recombinant-infected LCLs was consistently significantly smaller than that of B95-8 episomes (e.g., MG68, MG72, and MG76 in Fig. 10), while others were consistently similar than B95-8 or slightly larger (e.g., MG37, MG42, MG48, and MG65 in Fig. 10, and data not shown). While the size of EBV episomes can vary with the number of copies of the 3-kbp internal

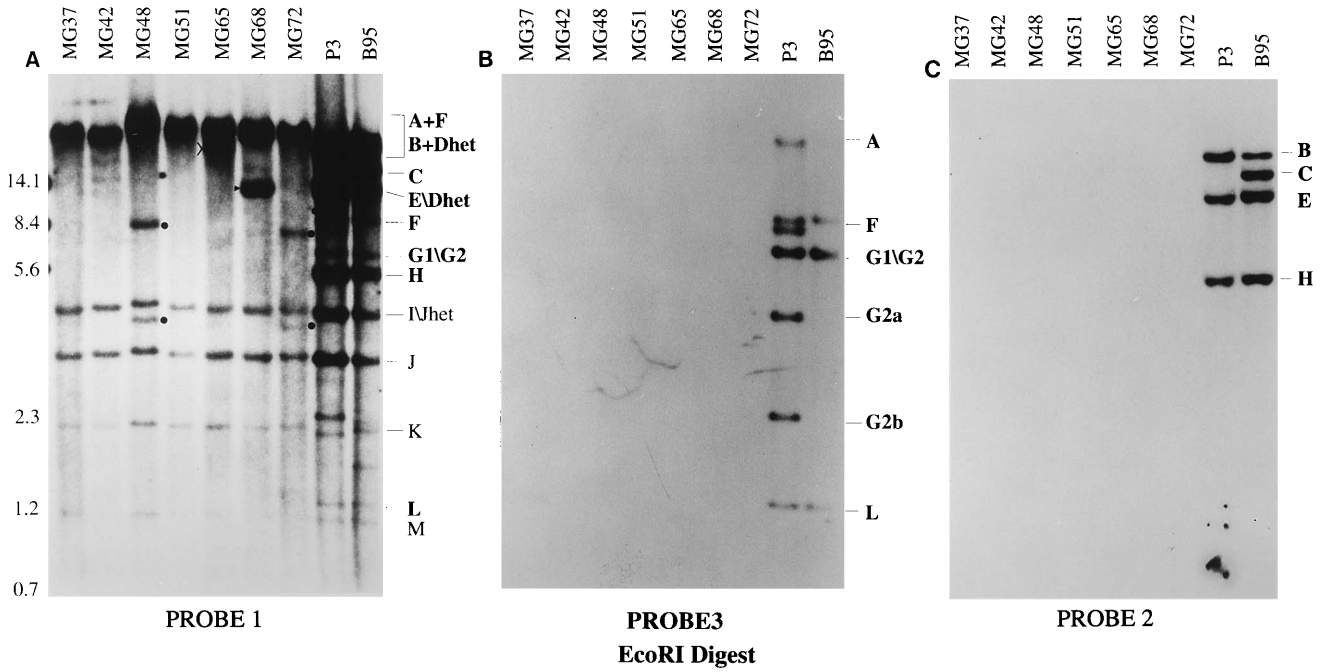

FIG. 7. Southern blot analysis of 30 μg of *Eco*RI-digested DNA from LCLs MG37 to MG72 infected with 18- and 58-kbp deletion mutant EBV recombinants. As controls, *Eco*RI-digested P3HR-1 and B95-8 cell DNAs (10 μg) are also shown. The DNA fragments were resolved on a 0.5% ME agarose gel. The 18-kbp deletion removes *Eco*RI G1, L, and G2 and part of *Eco*RI F and A (Fig. 1). P3HR-1 EBV has an extra *Eco*RI site in G2, resulting in G2a and G2b fragments. In the EBV recombinants, *Eco*RI F is fused to 46.6 kbp of the *Eco*RI A fragment (Fig. 1). The 58-kbp deletion joins the *Eco*RI-*Not*I fragment of *Eco*RI B to the *Not*I-*Sna*BI fragment of *Sna*BI B (33) (Fig. 1), resulting in deletion of the *Eco*RI E, H, and C fragments and fusion of the *Eco*RI B and Dhet fragments. (A) The EBV DNA fragments were identified by incubating the membrane with a [^{32}P]dCTP-labeled probe from the five cosmid-cloned fragments of EBV DNA (33). Individual fragments were identified by sequential stripping and probing with individual cosmid or plasmid EBV DNAs. Fragments affected by the deletions are labeled in boldface letters on the right of the blot. Anomalous fragments, identified by the solid circles, hybridize to an *Eco*RI A probe. The solid arrowhead indicates a fragment which hybridizes to a terminal repeat probe. The open arrow identifies a fragment which hybridizes to *Eco*RI B and *Sna*BI B but not to a terminal repeat probe. Lanes MG37 through MG72 are DNA fragments of the EBV recombinants deleted for the shaded regions shown in Fig. 1. Sizes are shown to the left (in kilobase pairs). (B) Hybridization to probe 3 (Fig. 1) made from the DNA fragments within the 18-kbp deletion. (C) Hybridization to probe 2, made from the 46-kbp deletion DNA obtained from a B95-8 cosmid (Fig. 1). The P3HR-1 *Eco*RI C fragment in panel C is 12 kbp larger than that in B95-8 and is indistinguishable from *Eco*RI B (Fig. 1).

repeat, the simplest model to explain the bimodal size variation observed in these experiments is that the smaller and larger episomes are, respectively, monomers or dimers of the doubly deleted EBV genome. The deletions remove genes essential for EBV DNA replication, and linear replicated EBV DNA is found only in the P3HR-1 and B95-8 cells (Fig. 10).

Immunoblot analyses of LCLs infected with EBV recombinants for EBNA, LMP1, and spontaneous lytic cycle EBV gene expression. Analysis of EBNA and LMP1 expression in LCLs infected with the doubly deleted EBV recombinants confirmed the expression of EBNA2, EBNA3A, EBNA3C, and EBNA1 of the size and type expected to be encoded by the transfected EBV DNA and not by P3HR-1 DNA (Fig. 11 and data not shown). The one exception was MG65, which had a smaller EBNA1, characteristic of P3HR-1 (Fig. 11). The abundance of the EBNAs and LMP1 is similar to that in B95 cells, which are frequently used as a control for WT-EBV-infected LCLs (Fig. 11 and data not shown). Thus, these data demonstrate that the deletions do not affect expression of the key genes for latent infection and cell growth transformation and that these genes were, with one exception, derived from the transfected DNA and not from P3HR-1 EBV DNA. Because the MG65 cell line had a P3HR-1-size EBNA1, MG65 DNA was also checked by PCR for the presence of type 1 or 2 EBNA3C DNA and was found to contain only type 1 EBNA3C. EBNA3C maps close to EBNA 1 (Fig. 1), and the presence of EBNA3C from the transfected DNA is evidence that recombination with the P3HR-1 genome was restricted to EBNA1. Thus, although almost completely derived from the transfected EBV cosmid DNA, the EBV recombinants with both deletions can incorporate a small segment from homologous P3HR-1 EBV DNA.

Although LMP1 expression in the double-deletion recombinant-EBV-infected LCLs is similar to that in WT-recombinant-infected LCLs, D1LMP is anomalously expressed in the double-deletion recombinant-infected LCLs (Fig. 11 and data not shown). D1LMP1 is a late lytic cycle gene and is usually not detected at this level in latently infected LCLs, including those that have the 58-kbp deletion (33). Thus, these data suggest that the double deletion results in a unique anomaly in D1LMP1 regulation.

LCLs transformed by the EBV recombinant genomes were similar to LCLs infected with WT EBV in their variable permissivity for expression of the BZLF1 immediate-early lytic replicative cycle protein (Fig. 12 and data obtained with a BZLF1-specific monoclonal antibody [not shown]). As expected, the p135 early DNA-binding protein is not expressed in LCLs infected with the EBV recombinants with both deletions, since the 58-kbp deletion removes this gene. Similarly, the abundant p45-55 (EA-D) early lytic proteins encoded by BMRF1 and BMLF1 are not expressed in these deletion-recombinant-infected LCLs because of the 18-kbp deletion, which includes these genes. The BZLF1 expression data indicate that the D1LMP1 expression observed in the LCLs infected with double-deletion recombinants is not a consequence of generally enhanced lytic cycle EBV gene expression.

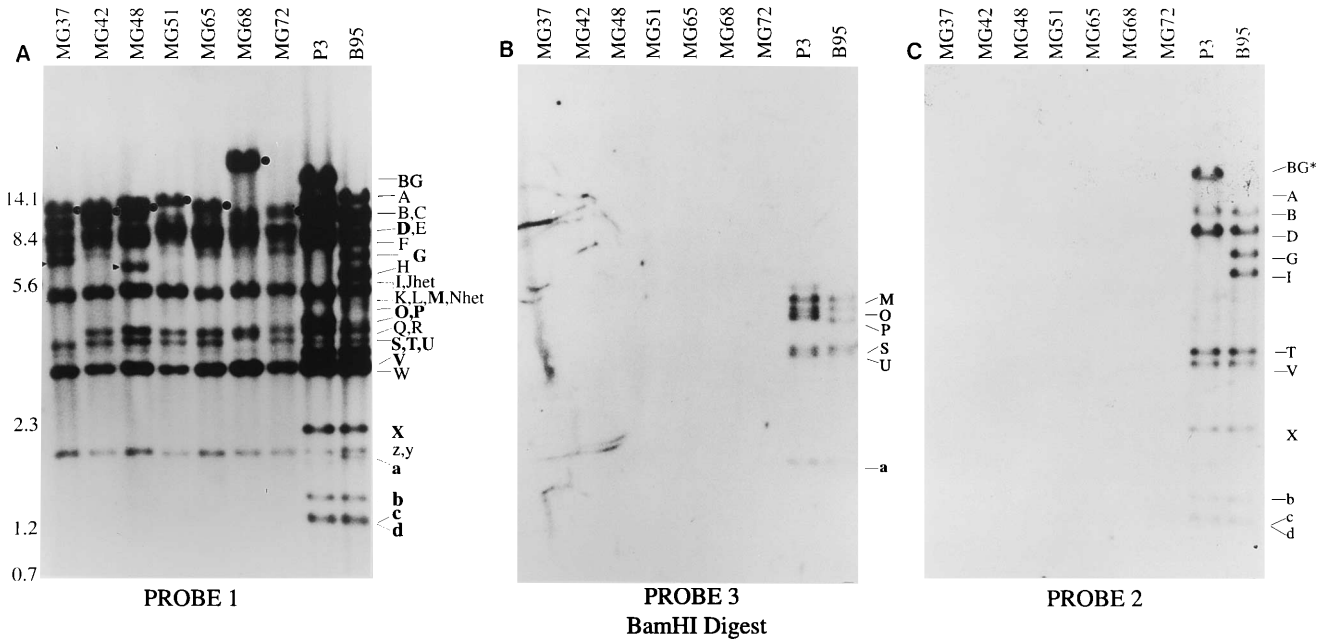

FIG. 8. Southern blot analyses of 30 μg of *Bam*HI-digested DNA from LCLs MG37 to MG72 infected with the EBV recombinant viruses deleted for the regions of the EBV genome shaded in Fig. 1. P3HR-1- and B95-8-infected cell DNAs (10 μg) are included as controls. Fragments were resolved on a 0.5% ME agarose gel. (A) The probe was a mixture of the five cosmid EBV DNAs (45). Fragments were identified by stripping the blot and then probing sequentially with probes made from each of the three transfected cosmids or from an *Mlu*I-*Eco*RI fragment containing the terminal repeats. The solid circles on the right of each lane identify a fragment in each of the LCL DNAs which hybridizes to a probe made from the terminal repeats. The arrow on the left indicates a 7.5-kbp fragment in lane MG37 which is due to the loss of the Q/U *Bam*HI site. The arrow to the left of the MG48 lane indicates an anomalous fragment which is specifically identified with the ESN probe and is therefore part of *Sal*I EC, which is not affected by the 18-kbp deletion. Sizes are shown to the left (in kilobase pairs). (B) Probe 3 is the 18-kbp-deleted DNA. (C) Probe 2 is the 46-kbp-deleted DNA from the B95-8 DNA (Fig. 1). The 18-kbp deletion probe 3 hybridizes to P3HR-1 and B95-8 *Bam*HI fragments M, O, P, S, and U in panel B, and the 46-kbp deletion probe 2 hybridizes to *Bam*HI fragments BG* (P3HR-1 only), A, B, D, G, I, T, V, X, B, C, and d of P3HR-1 and B95-8, as indicated in panel C (see Fig. 1).

DISCUSSION

These experiments confirm and extend previous observations (33) that transforming EBV recombinants carrying large deletions can be constructed by transfecting overlapping large EBV DNA fragments that include a lytic DNA replication origin and a packaging signal into cells harboring a lytic replication-competent EBV genome which can provide replication functions in *trans*. Transforming, replication-defective mini-EBV genomes are produced by homologous recombination among the transfected EBV DNAs, and other, mostly larger, transforming genomes are produced by homologous recombination of the transfected DNAs with the endogenous P3HR-1 genome. More than 20% of the recombinants appear to comprise solely the transfected cosmid DNA. These 18- and 58-kbp-deleted recombinants lack the deleted DNA, as shown by Southern blot with probes composed of the deleted DNAs and by PCR tests, which exclude the presence of eight different components of the deleted DNA in at least 99% of the transformed cells.

While we cannot rigorously exclude the possibility that P3HR-1 coinfection may have contributed to the initial transformation of the primary B lymphocytes and have been unnecessary for maintenance of transformation, that possibility is unlikely. The LCLs were first screened for the presence of P3HR-1 DNA at 4 weeks after infection, a time at which transformed-cell outgrowth is first obvious. Second, P3HR-1 coinfection, when initially present, is usually maintained for several months of cell growth. Third, the minirecombinant-infected LCLs became recognizable as transformed foci and continued to grow similarly to WT recombinants derived in parallel. Fourth, these transformants were derived and passaged without the benefit of fibroblast feeder layers which could otherwise support the growth of partially transforming EBV recombinants (25).

The dispensability of the largest EBNA intron for primary B-lymphocyte growth transformation is a surprising finding, perhaps even more surprising than the dispensability of most of the genome between EBNA1 and LMP1. EBNA expression must be tightly regulated in LCLs at the level of RNA processing, since all of the EBNA mRNAs are transcribed by a single promoter. This long intron could have been important in differential processing of the EBNA mRNAs. The splice donor site at the beginning of the intron is only 1 kbp from the deletion, and its function could have been affected. At least three alternative acceptor sites downstream of the deletion must be recognized in a regulated fashion, since EBNA3A and -3C and EBNA1 are all essential or critical for LCL outgrowth (3, 4, 9, 34, 35, 44). EBNA expression was unaffected by the deletions. If the EBNA introns and noncoding exons turn out to be entirely deletable, balanced expression of the EBNA mRNAs would likely be attributable to differential polyadenylation rather than splicing. Also, the deletion of 18 and 58 kbp of EBV DNA might interfere with packaging, since a reconstituted genome of 60 to 90 kbp is about 40 to 50% of the size of a complete EBV genome. Our data on this issue are limited, based on the Southern analysis and in situ lysis gels, but suggest that some recombinants may have been packaged as monomers and others as dimers. Overall, any negative effects on packaging are offset by the efficiency of recombination among the three transfected cosmid DNAs.

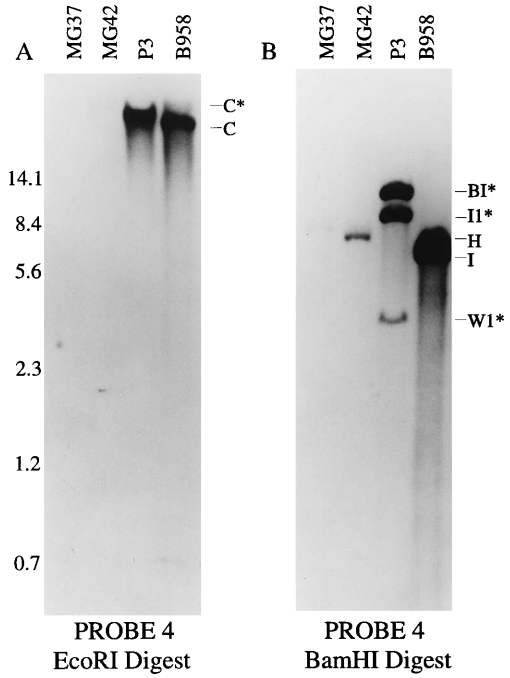

FIG. 9. Southern blot analysis of the *Eco*RI and *Bam*HI DNA fragments (30 μg) prepared from MG37 and MG42 recombinant-infected cell lines or from P3HR-1 and B95-8 cell DNAs (10 μg) probed with labeled *Bam*HI B1, I1, and W1, which comprise the 12 kbp of DNA deleted from the B95-8 genome and the B95-8 *Bam*HI I fragment (see Fig. 1). The DNAs were resolved on a 0.5% ME agarose gel, transferred to a nylon membrane, and incubated with [^{32}P]dCTP-labeled *Bam*HI B1, I1, and W1 (probe 4 in Fig. 1). On longer exposures, some hybridization is evident to *Eco*RI A and to *Bam*HI H of MG37 and MG42 because of homology between *Bam*HI B1 and *Bam*HI H (12) (Fig. 1). Sizes are shown to the left (in kilobase pairs).

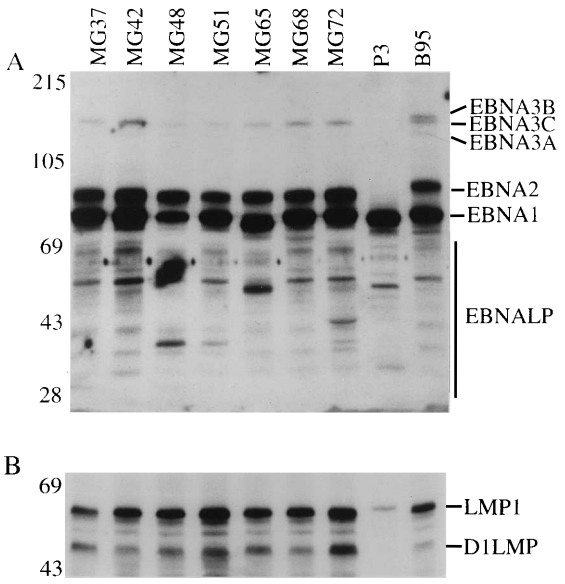

FIG. 11. Immunoblot analysis of EBNA and LMP1 expression in 18- and 58-kbp-deleted EBV-recombinant-infected LCLs MG37 to MG72. Type 2 P3HR-1- and type 1 B95-8-infected cells are included as controls. The proteins were analyzed on SDS–8% PAGE gels, transferred to nitrocellulose, and incubated with a 1:50 dilution of a human serum which identifies EBNA1 and the type 1 EBNA2, EBNA3A, -3B, and -3C proteins and weakly reacts with type 2 EBNA3A, -3B, and -3C. (A) All the LCLs infected with the minimal transforming genome express B95-8 EBNAs except for LCL MG65, which has a P3HR-1-size EBNA 1. (B) Immunoblot incubated with the S12 monoclonal antibody to LMP1 (24). All the 18- and 58-kbp deletion recombinant-infected LCLs express LMP1 and D1LMP1. The size markers are indicated on the left (in kilodaltons).

The only anomaly observed in latent EBV gene expression in the LCLs infected with the 18- and 58-kbp-deleted recombinants was expression of D1LMP1, which was unusually high in these mini-EBV genomes, possibly because of the deletion of a *cis*-acting regulatory element for D1LMP1 expression. D1LMP1 is a form of LMP1 that is ordinarily expressed late in lytic infection. In rodent fibroblasts, D1LMP1 has no transforming effects and does not inhibit LMP1-mediated transformation (19, 22). Consistent with the rodent fibroblast experiments, D1LMP1 expression had no adverse effect on the growth of cells transformed by the 18- and 58-kbp-deleted EBV recombinants.

Incorporation of small segments of homologous DNAs from the endogenous P3HR-1 genome occurred in these experiments, although it was infrequent. Nonhomologous recombination was unusual, as in previous experiments of this type (33, 40–45). From the results in these and previous experiments, recombination with the endogenous P3HR-1 genome is unlikely to occur near sites of nonhomology, such as pertains when the transfected DNA is deleted for a large segment (33).

The fraction of recombinants arising from among the transfected DNAs is higher in this and in the previous three cosmid transfection than in the experiments with all five WT EBV DNA fragments (33, 45). The increased frequency of recombinants from the transfected DNAs is probably due to the less complex interactions necessary for recombination among three instead of five transfected DNA fragments. If so, the efficiency can probably be improved by cloning the transfected DNA fragments into two cosmids. Pulsed-field gel electrophoresis of the *Eco*RI A fragment indicates a size of 47 kbp, probably due to a reduction in the copy number of the 3-kbp internal repeat to six (Fig. 1). As a result of recombination with the deleted *Sal*I EC and *Eco*RI B-*Sna*BI B fragments, 0.2 kbp is deleted from the end of *Eco*RI A and DNA corresponding to bp 87030 to 117609 and bp 1 to 7315 is added, bringing the total recombinant size to 93 kbp. Other deletions in DNA encoding the EBERs, LMP2, BCRF1, and BHRF1 have been made without affecting primary B-lymphocyte growth transformation (23, 26,

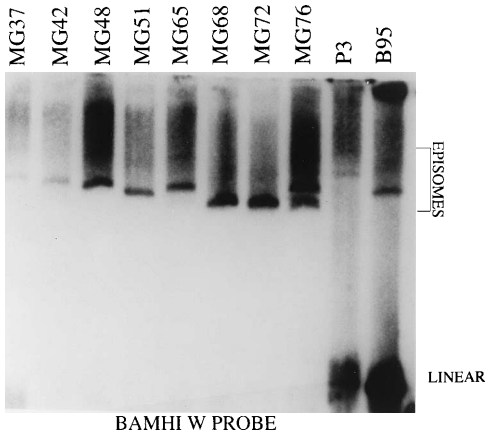

FIG. 10. Southern blot analysis of EBV episomes analyzed by electrophoresis on a 0.75% ME agarose in situ lysis gel (10). The probe was made from the EBV *Bam*HI W fragment. Lanes MG37 through MG76 are DNAs released from the EBV recombinant (deleted for 18 kbp and 58 kbp)-infected LCLs. P3 and B95 are DNAs from EBV-infected P3HR-1 and B95-8 cells, respectively.

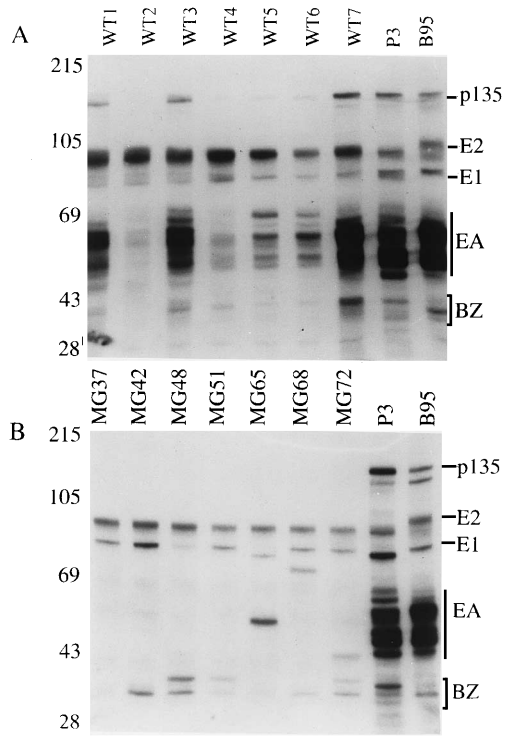

FIG. 12. Immunoblot analysis of lytic EBV proteins in LCLs infected with 18- and 58-kbp-deleted EBV recombinants. The blots were incubated with a 1:50 dilution of a human immune serum which identifies EBNA1, type 1 EBNA 2, the 45- to 55-kDa BMRF1 and BMLF1 EA-D complex, the early lytic 135-kDa BALF2 single-stranded-DNA-binding protein, and the BZLF1 immediate-early protein. BZLF1 was also identified with a BZLF1 monoclonal antibody (data not shown). (A) Proteins from seven WT recombinant-infected LCLs derived in the same transfection and transformation experiment. (B) Analysis of proteins from LCLs MG37 to MG72 infected with the EBV recombinants. Proteins from P3HR-1 (P3) and B95-8 (B95) cells are shown as controls.

40, 41). Together with the previous experiments, the current experiments demonstrate that the unique EBV DNA required for B-lymphocyte transformation is less than 64 kbp. The experiments also raise the possibility that DNA that encodes other EBNA introns and noncoding exons can also be deleted. Thus, a reduction in the complexity of the transforming EBV genome to the size of two cosmids is feasible, and a reduction to even one cosmid clone may be possible.

Improvements in this recombinant EBV molecular genetic strategy are important for several reasons. First, they enable exclusion of large segments of the genome from being critical to the maintenance of latent infection and cell growth transformation. Second, these transfected EBV DNA fragments are propagated as high-copy *E. coli* plasmids, amenable to molecular genetic alterations. Specific mutations can be engineered in the plasmid DNAs so that the importance of domains of critical genes can be assayed by creating novel EBV recombinants in transfected P3HR-1 cells. Third, the *E. coli*-cloned deleted EBV DNA fragments may be suitable for the construction of transforming, replication-defective EBV recombinants carrying large segments of heterologous DNA. Autologous lymphocytes transformed by replication-defective EBV may be useful for gene therapy or for immunotherapy. Such vector-host systems might be useful for the self-regulated expression in vivo of large segments of human DNA, enabling the preservation of endogenous regulatory elements. Strategies can be envisaged for the biological, immunological, pharmacological, or physical containment of such cells in humans.

ACKNOWLEDGMENTS

This research was supported by research grant CA47006 from the National Cancer Institute of the Public Health Service. E.R. is a fellow of the Cancer Research Institute.

Xue-Quian Miao and Lisa Vara contributed excellent technical assistance. Blake Tomkinson contributed to the discussions of the data and provided helpful hints.

REFERENCES

1. **Baer, R., A. Bankier, M. Biggen, P. Deininger, P. Farrell, T. Gibson, G. Hatfull, G. Hudson, S. Satchwell, C. Sequin, P. Tuggnell, and B. Barrell.** 1984. DNA sequence and expression of the B95-8 Epstein-Barr genome. Nature (London) **310:**207–211.
2. **Bodescot, M., B. Chambraud, P. Farrell, and M. Perricaudet.** 1984. Spliced RNA from the IRI-U2 region of Epstein-Barr virus: presence of an opening reading frame for a repetitive polypeptide. EMBO J. **3:**1913–1917.
3. **Bodescot, M., and M. Perricaudet.** 1986. Epstein-Barr virus mRNAs produced by alternative splicing. Nucleic Acids Res. **17:**7130–7134.
4. **Bodescot, M., M. Perricaudet, and P. J. Farrell.** 1987. A promoter for the highly spliced EBNA family of RNAs of Epstein-Barr virus. J. Virol. **61:** 3424–3430.
5. **Cleary, M. L., R. F. Dorfman, and J. Sklar.** 1986. Failure in immunological control of virus infection: post transplant lymphomas, p. 163–181. *In* M. A. Epstein and B. G. Achong (ed.), The Epstein-Barr virus: recent advances. William Heinemann Medical Books Ltd., London.
6. **Cohen, J. I., F. Wang, and E. Kieff.** 1991. Epstein-Barr virus nuclear protein 2 mutations define essential domains for transformation and transactivation. J. Virol. **65:**2545–2554.
7. **Cohen, J. I., F. Wang, J. Mannick, and E. Kieff.** 1989. Epstein-Barr virus nuclear protein 2 is a key determinant of lymphocyte transformation. Proc. Natl. Acad. Sci. USA **86:**9558–9562.
8. **Countryman, J., H. Jenson, R. Seibl, H. Wolf, and G. Miller.** 1987. Polymorphic proteins encoded within BZLF1 of defective and standard Epstein-Barr viruses disrupt latency. J. Virol. **61:**3672–3679.
9. **Farrell, P.** 1993. Epstein-Barr virus, p. 1.120–1.133. *In* S. J. O'Brien (ed.), Genetic maps. Cold Spring Harbor Laboratory, Cold Spring Harbor, N.Y.
10. **Gardella, T., P. Medveczky, T. Sairenji, and C. Mulder.** 1984. Detection of circular and linear herpesvirus DNA molecules in mammalian cells by gel electrophoresis. J. Virol. **50:**248–254.
11. **Hammerschmidt, W., and B. Sugden.** 1989. Genetic analysis of immortalizing functions of Epstein-Barr virus in human B lymphocytes. Nature (London) **340:**393–397.
12. **Heller, M., T. Dambaugh, and E. Kieff.** 1981. Epstein-Barr virus DNA. IX. Variation among viral DNAs from producer and nonproducer infected cells. J. Virol. **38:**632–648.
13. **Heller, M., V. van Santen, and E. Kieff.** 1982. A simple repeat sequence in Epstein-Barr virus DNA is transcribed in latent and productive infection. J. Virol. **44:**311–320.
14. **Henderson, A., S. Ripley, M. Heller, and E. Kieff.** 1983. Human chromosome association of Epstein-Barr virus DNA in a Burkitt tumor cell line and in lymphocytes growth transformed *in vitro*. Proc. Natl. Acad. Sci. USA **80:** 1987–1991.
15. **Henle, W., V. Diehl, G. Kohn, H. zur Hausen, and G. Henle.** 1967. Herpes type-virus and chromosome marker in normal leukocytes after growth with irradiated Burkitt's cells. Science **157:**1064–1065.
16. **Heston, L., M. Rabson, N. Brown, and G. Miller.** 1982. New Epstein-Barr virus variants from cellular subclones of P3J-HR-1 Burkitt lymphoma. Nature (London) **295:**160–163.
17. **Jeang, K. T., and S. D. Hayward.** 1983. Organization of one Epstein-Barr virus molecule. III. Location of one P3HR-1 deletion junction and characterization of the *Not*I repeat units that form part of the template for an abundant 12-*O*-tetradecanoyl phorbol-13-acetate mRNA transcript. J. Virol. **48:**135–148.
18. **Joab, I., D. T. Rowe, M. Bodescot, J. C. Nicolas, P. J. Farrell, and M. Perricaudet.** 1987. Mapping of the gene coding for Epstein-Barr virus-determined nuclear antigen EBNA 3 and its transient overexpression in a human cell line by using an adenovirus expression vector. J. Virol. **61:**3340–3344.
19. **Kaye, K., K. Izumi, and E. Kieff.** 1993. An integral membrane protein is essential for Epstein-Barr virus transformation of primary B lymphocytes. Proc. Natl. Acad. Sci. USA **90:**9150–9154.
20. **Kieff, E., K. Izumi, K. Kaye, R. Longnecker, J. Mannick, C. Miller, E. Robertson, S. Swaminathan, B. Tomkinson, X. Tong, and R. Yalamanchili.** 1994. Specifically mutated Epstein-Barr virus recombinants: defining the minimal genome for primary B lymphocyte transformation, p. 123–147. *In* A. Minson, J. Neil, and M. McCare (ed.), Viruses and cancer (Symposia of the

Society for General Microbiology). Cambridge University Press, Cambridge.
21. **King, W., T. Dambaugh, M. Heller, J. Dowling, and E. Kieff.** 1982. Epstein-Barr Virus (EBV) DNA. XII. A variable region of the EBV genome is included in one P3HR-1 deletion. J. Virol. **43:**979–986.
22. **Liebowitz, D., and E. Kieff.** 1993. Epstein-Barr virus, p. 107–173. *In* B. Roizman, R. Whitley, and C. Lopez (ed.), The human herpes viruses. Raven Press, New York.
23. **Longnecker, R., C. L. Miller, B. Tomkinson, X. Miao, and E. Kieff.** 1993. Deletion of DNA encoding the first five transmembrane domains of the Epstein-Barr virus latent membrane proteins 2A and 2B. J. Virol. **67:**5068–5074.
24. **Mann, K. P., D. Staunton, and D. Thorley-Lawson.** 1985. Epstein-Barr virus-encoded protein found in plasma membranes of transformed cells. J. Virol. **55:**710–720.
25. **Mannick, J., J. I. Cohen, M. Birkenbach, A. Marchini, and E. Kieff.** 1991. The Epstein-Barr virus nuclear protein encoded by the leader or the EBNA RNAs (EBNA-LP) is important in B lymphocyte transformation. J. Virol. **65:**6826–6837.
26. **Marchini, A., B. Tomkinson, J. Cohen, and E. Kieff.** 1991. BHRF1, the Epstein-Barr virus gene with homology to bcl-2, is dispensable for B-lymphocyte transformation and virus replication. J. Virol. **65:**5991–6000.
27. **Matsuo, T., M. Heller, L. Petti, E. Oshiro, and E. Kieff.** 1984. Persistence of the entire EBV genome integrated into human lymphocyte DNA. Science **226:**1322–1325.
28. **Miller, G., J. Robinson, L. Heston, and M. Lipman.** 1974. Differences between laboratory strains of Epstein-Barr virus based on immortalization, abortive infection, and interference. Proc. Natl. Acad. Sci. USA **71:**4006–4010.
29. **Miller, G., T. Shoppe, H. Lisco, D. Stitt, and M. Lipman.** 1972. Epstein-Barr virus: transformation, cytopathic changes, and viral antigens in squirrel monkey and marmoset leukocytes. Proc. Natl. Acad. Sci. USA **69:**383–387.
30. **Mosier, D., R. Gulizia, S. Baird, and D. Wilson.** 1988. Transfer of a functional human immune system to mice with severe combined immunodeficiency. Nature (London) **335:**256–259.
31. **Nilsson, K., G. Klein, W. Henle, and G. Henle.** 1971. The establishment of lymphoblastoid lines from adult and fetal human lymphoid tissue and its dependence on EBV. Int. J. Cancer **8:**443–450.
32. **Pope, J. H., B. Achong, and M. Epstein.** 1968. Cultivation and pure structure of virus bearing lymphoblasts from 2nd, N. G. Burkitt lymphoma. Int. J. Cancer **3:**171–182.
33. **Robertson, E., B. Tomkinson, and E. Kieff.** 1994. An Epstein-Barr virus with a 58-kilobase-pair deletion that includes BARF0 transforms B lymphocytes in vitro. J. Virol. **68:**1449–1458.
34. **Sample, J., M. Hummel, D. Braun, M. Birkenbach, and E. Kieff.** 1986. Nucleotide sequences of mRNAs encoding Epstein-Barr virus nuclear proteins: a probable transcriptional initiation site. Proc. Natl. Acad. Sci. USA **83:**5096–5100.
35. **Sample, J., and E. Kieff.** 1990. Transcription of the Epstein-Barr virus genome during latency in growth-transformed lymphocytes. J. Virol. **64:**1667–1674.
36. **Sample, J., L. Young, B. Martin, T. Chatman, E. Kieff, A. Rickinson, and E. Kieff.** 1990. Epstein-Barr virus types 1 and 2 differ in their EBNA3A, EBNA3B, and EBNA3C genes. J. Virol. **64:**4084–4092.
37. **Shope, T., D. Dechairo, and G. Miller.** 1973. Malignant lymphoma in cotton top marmosets after inoculation with Epstein-Barr virus. Proc. Natl. Acad. Sci. USA **70:**2487–2491.
38. **Skare, J., J. Farley, J. L. Strominger, K. O. Fressen, M. S. Cho, and H. zur Hausen.** 1985. Transformation by Epstein-Barr virus requires sequences in the region of *Bam*HI fragments Y and H. J. Virol. **55:**286–297.
39. **Speck, S., and J. Strominger.** 1985. Analysis of the transcript encoding the latent Epstein-Barr virus nuclear antigen 1: a potentially polycistronic message generated by long range splicing of several exons. Proc. Natl. Acad. Sci. USA **82:**8305–8309.
40. **Swaminathan, S., R. Hesselton, J. Sullivan, and E. Kieff.** 1993. Epstein-Barr virus recombinants with specifically mutated BCRF1 genes. J. Virol. **67:**7406–7413.
41. **Swaminathan, S., B. Tomkinson, and E. Kieff.** 1991. Recombinant Epstein-Barr virus with small RNA (EBERS) genes deleted transforms lymphocytes and replicates in vitro. Proc. Natl. Acad. Sci. USA **88:**1546–1550.
42. **Tomkinson, B., and E. Kieff.** 1992. Second-site homologous recombination in Epstein-Barr virus: insertion of type 1 EBNA 3 genes in place of type 2 has no effect on in vitro infection. J. Virol. **66:**780–789.
43. **Tomkinson, B., and E. Kieff.** 1992. Use of second-site recombination to demonstrate that Epstein-Barr virus nuclear protein 3B is not important for lymphocyte infection or growth transformation in vitro. J. Virol. **66:**2893–2903.
44. **Tomkinson, B., E. Robertson, and E. Kieff.** 1993. Epstein-Barr virus nuclear proteins EBNA3A and EBNA3C are essential for B-lymphocyte growth transformation. J. Virol. **67:**2014–2025.
45. **Tomkinson, B., E. Robertson, R. Yalamanchili, and E. Kieff.** 1993. Epstein-Barr virus recombinants from overlapping cosmid fragments. J. Virol. **67:**7298–7306.
46. **van Santen, V., A. Cheung, M. Hummel, and E. Kieff.** 1983. RNA encoded by the IR1-U2 region of Epstein-Barr virus DNA in latently infected growth-transformed cells. J. Virol. **46:**424–433.
47. **Yates, J. L., N. Warren, and B. Sugden.** 1985. Stable replication of plasmids derived from Epstein-Barr virus in various mammalian cells. Nature (London) **313:**812–815.